RSC Advances

ROYAL SOCIETY OF CHEMISTRY

www.rsc.org/advances

Graphical Abstract

Emission and surface properties of main-chain type polybenzoxazine with pyridinyl moieties

Ching Hsuan Lin,* Yu Sin Shih, Meng Wei Wang, Chun Yu Tseng, Tzong Yuan Juang, Chih Feng Wang*

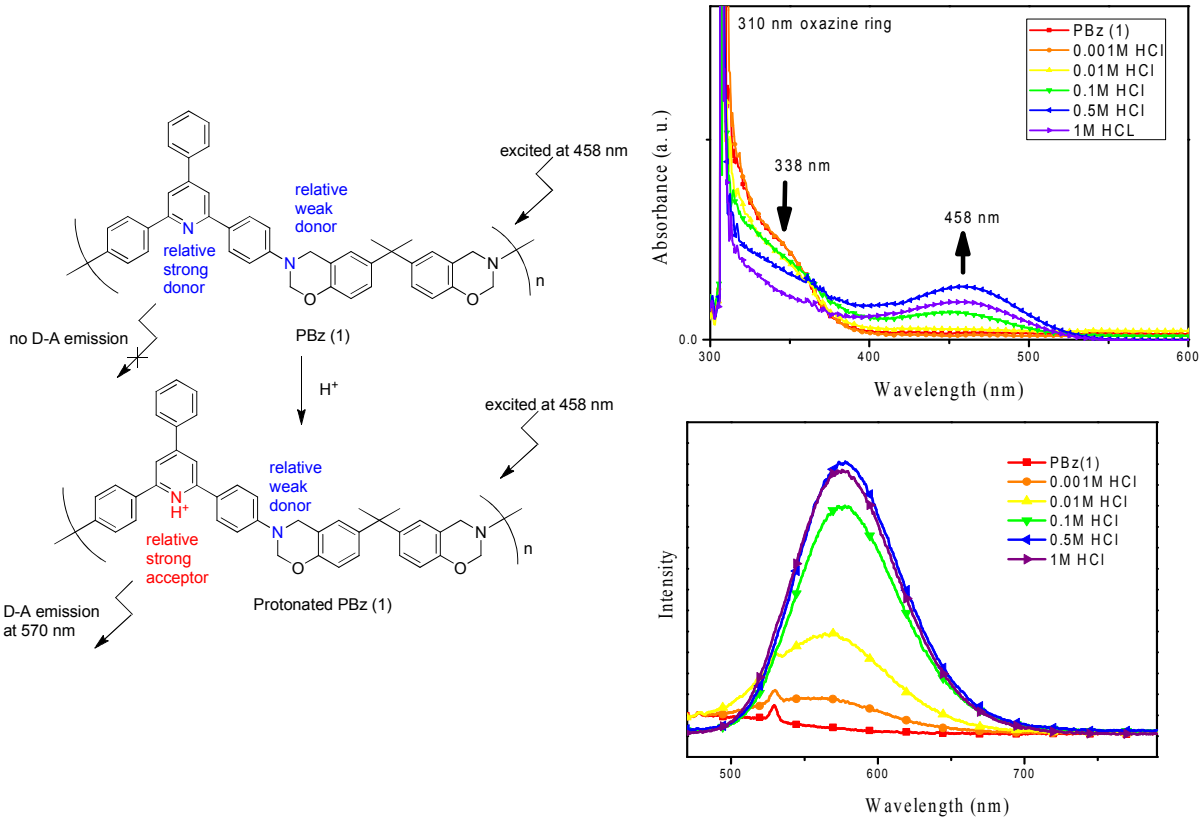

A main-chain type polybenzoxazine, PBz **(1),** with pyridinyl moieties was prepared. When the THF dilute solution of PBz **(1)** was protonated with HCl, a new absorption at 458 nm was observed in the UV-vis spectrum. After being excited at 458 nm, a strong emission at 570 nm was observed in the fluorescence spectrum. This result suggests that the pyridinyl-containing PBz (1) can be used as a proton sensor via a protonation process.

Emission and surface properties of main-chain type polybenzoxazine with pyridinyl moieties

Ching Hsuan Lin,*[a] Yu Sin Shih,[a] Meng Wei Wang,[a] Chun Yu Tseng,[a] Tzong Yuan Juang,[b] Chih Feng Wang*[c]

[a] Department of Chemical Engineering, National Chung Hsing University, Taichung, Taiwan

[b] Department of Applied Chemistry, National Chiayi University, Chiayi, Taiwan

[c] Department of Materials Science and Engineering, I-Shou University, Kaohsiung, Taiwan

Abstract

A main-chain type polybenzoxazine, PBz **(1),** with pyridinyl moieties was successfully synthesized from the Mannich condensation of 4-phenyl-2,6-bis(4-aminophenyl) pyridine **(2)**, paraformaldehyde, and bisphenol A. For the purpose of property comparison, a structurally similar polybenzoxazine, PBz **(2)**, was prepared. Unfortunately, PBz **(2)** is insoluble in organic solvents due to its rigid structure. In contrast, the pyridinyl group provided solubility for the processing of PBz **(1)**. When the THF dilute solution of PBz **(1)** was protonated with HCl, a new absorption at 458 nm was observed in the UV-vis spectrum. No emission at 500-700 nm occurred in the fluorescence spectrum before protonation of PBz **(1)**. However, upon protonation, the protonated pyridinyl became a stronger acceptor, and then, an emission at 570 nm occurred between the nitrogen of benzoxazine (donor) and protonated pyridinyl groups (acceptor) after being excited at 458 nm. After thermal curing, the thin film of PBz **(1)** thermoset was flexible, with a T_g value at 261 ^oC, a coefficient of thermal expansion 38 ppm/^oC, and 5% decomposition temperature at 414 (N_2) and 419 ^oC (air). The contact angle is as high as 102^o, and the surface energy is as low as 19.6 mJ/m^2.

Introduction

Pyridine, with a localized lone pair of electrons on the nitrogen atom, is an aromatic heterocycle that can enhance solubility. Recently, some reports have been concerned with the introduction of pyridinyl groups into polymer to increase thermal stability due to the molecular symmetry and aromaticity of pyridine.[1-6] Pyridine-containing amines are generally prepared by the Chichibabin reaction[7-10] and the modifided Chichibabin reaction.[11] The modified Chichibabin reaction has been used to prepared pyridine-containing diamines, 4-aryl-2,6-bis(4-aminophenyl) pyridines.[1] Polyamides[1] and polyimides[3] based on the pyridine-containing diamines show good thermal stability and solubility in polar aprotic solvents. Pyridine-containing diamine with a diphenoxy structure, 4-phenyl-2,6-bis[4-(4-aminophenoxy)phenyl]-pyridine, has been prepared to prepare polyimide with transparency, flexibility and solubility.[5] Pyridine-containing diamines with a naphthalene or pyrene moiety have been reported by Liaw et al.[6] Polyimides with good thermal stability, mechanical properties and high dielectric constant were prepared based on the diamines. Liaw and Wang et al. prepared pyridine-containing diamines with a triphenylamine structure and discussed its emission after protonation.[2, 6, 12, 13]

Benzoxazines are resins that can be polymerized to thermosets by means of thermally activated ring-opening reactions.[14-16] Thermosets with low water absorption, superior electrical properties[17] and low surface energy[18] can be obtained after curing. Main-chain-type polybenzoxazines are an active concept in the recent development of benzoxazines. They can be prepared by Mannich-type polycondensation of diamine, bisphenol, and formaldehyde.[19-23] However, most of the discussion on properties focuses on the thermal and mechanical properties of benzoxazine thermosets. UV-vis absorption and emission characteristics of polybenzoxazines have never been reported. In this work, a main-chain type polybenzoxazines, PBz **(1)**, with pyridinyl moieties was successfully synthesized from the Mannich condensation of 4-phenyl-2,6-bis(4-aminophenyl) pyridine **(2)**, paraformaldehyde, and bisphenol A. For the purpose of property comparison, a structurally similar polybenzoxazine,

PBz **(2)**, was also prepared. Detailed synthesis, absorption and emission of PBz **(1)** upon protonation, surface energy and thermal properties of PBz **(1)** thermoset are provided in this work.

Experimental

Materials. Benzaldehyde, bisphenol A and paraformaldehyde were purchased from TCI. Phenol, ammonium acetate, and hydrazine hydrate 80%were purchased form Showa. Palladium on carbon 10 %, p-nitroacetophenone were purchased from Acros. Glacial acetic acid and acetic anhydride were purphased from Scharlau. Boron trifluoride diethyl etherate was purchased from ALFA. All solvents were HPLC grade and were purchased from Tedia. P(B-oda) is a main-chain type polybenzoxazine prepared from 4,4'-diamino diphenyl methane/phenol/paraformaldehyde according our previous work.[24]

Preparation of diamine (2). Diamine **(2)** was prepared by a two-step procedure (Scheme 1)[1], and the procedure is listed in supporting information.

Preparation of diamine (5). Diamine **(5)** was prepared by a three-step procedure (Scheme S1)[25], and the procedure is listed in supporting information.

Synthesis of PBz (1) and PBz (2). PBz **(1)** was prepared by a one-pot procedure (Scheme 1). **(2)** 20.00 g (0.059 mole), bisphenol A 13.53 g (0.059 mole), paraformaldehyde 7.12 g (0.236 mole), and a mixed solvent of toluene/ethanol 120 mL (1/1, V/V) were introduced into a round-bottom 500 mL glass flask equipped with a nitrogen inlet, a condenser, and a magnetic stirrer. The reaction mixture was stirred at 80 ^{o}C for 24 h. After that, the solution was poured into methanol. The precipitate was filtered and dried in a vacuum oven. Yellow powder (85 % yield) was obtained. PBz **(2)** was similarly prepared except the starting diamine was **(5)**. Yellow powder (90 % yield) was obtained.

Preparation of PBz (1) thermoset for thermal property measurement. A 25 wt% PBz **(1)** in NMP solution was prepared. The solution was then cast onto glass by an automatic film applicator. The resulting films were transparent and colorless. They were dried at 60 ^{o}C overnight and cured at

100 ^{o}C (1 h), 160 ^{o}C (1 h), 200 ^{o}C (1 h) and 240 ^{o}C (1 h), respectively. After that, brown transparent films (about 60 um) were obtained by soaking the coated glass in water. The sample ID of the film of PBz **(1)** thermoset is named PBz **(1)**-T.

Thin-Film Formation for contact angle measurement. A polymer stock solution was prepared by dissolving the polybenzoxazine precursor in THF at a concentration of 30 mg mL^{-1}. The solution was filtered through a 0.2 μm syringe filter before spin-coating onto a glass slide (50 × 50 × 1 mm). 1 mL of the appropriate polymer solution was spin-coated onto a glass slide using a photoresist spinner operating at 1500 rpm for 45 s. The sample was left to dry at 60 °C for 1 h, and then it was cured in an oven at a desired time under 240 °C.

Characterization. Differential scanning calorimetry (DSC) was performed using a Perkin-Elmer DSC 7 in a nitrogen atmosphere at a heating rate of 10 min/^{o}C. Thermal gravimetric analysis (TGA) was performed with a Perkin-Elmer Pyris1 at a heating rate of 20 ^{o}C/min in a nitrogen or air atmosphere. Dynamic mechanical analysis (DMA) was performed with a Perkin-Elmer Pyris Diamond DMA with a sample size of 5.0x1.0x0.006 cm. The storage modulus E' and tan δ were determined as the sample was subjected to the temperature scan mode at a programmed heating rate of 5 ^{o}C/min at a frequency of 1Hz. The test was performed by a bending mode with an amplitude of 25 μm. Thermal mechanical analysis (TMA) was performed with a Perkin-Elmer Pyris Diamond TMA at a heating rate of 5 ^{o}C/min. The coefficient of thermal expansion was recorded in the temperature range of 50 ^{o}C to 150 ^{o}C. NMR measurements were performed using a Varian Inova 600 NMR in DMSO-d_6, and the chemical shift was calibrated by setting the chemical shift of DMSO-d_6 as 2.49 ppm. IR Spectra were obtained from at least 32 scans in the standard wavenumber range of 400–4000 cm^{-1} by a Perkin-Elmer RX1 infrared spectrophotometer. Gel permeation chromatography (GPC) was carried out on a Perkin-Elmer series 200a using THF as the eluent at 25 ^{o}C with a flow rate of 1.0 mL/min. The data were calibrated with polystyrene standard. UV-vis spectrum was performed by a Shimadzu UV mini 1240 spectrophotometer. Fluorescence spectrum was performed

by a Hitachi F-2500 spectrophotometer. The concentration of polybenzoxazine in THF is 0.01M for both UV and Fluorescence spectrum. The contact angle of the polymer sample was measured at 25 °C using a FDSA MagicDroplet-100 contact angle goniometer interfaced with image-capture software by injecting a 5 μL liquid drop. To obtain reliable contact data, at least three droplets were in at different regions of the same piece of film, and at least two pieces of film were used to obtain reliable contact angle data. Thus, at least six advancing contact angles were averaged for each type of film and each kind of liquid. Deionized water, ethylene glycol, and diiodomethane were used as standards to measure the surface free energies.

Results and discussion

Synthesis of PBz (1). Diamine **(2),** a precursor for PBz **(1)**, was prepared by a modified Chichibabin reaction, followed by reduction.[1] Figure S1 shows the ^{1}H-NMR of **(2)**. The signals are consistent with the structure. PBz **(1)** was prepared from the Mannich condensation of **(2)**, paraformaldehyde, and bisphenol A (Scheme 1).

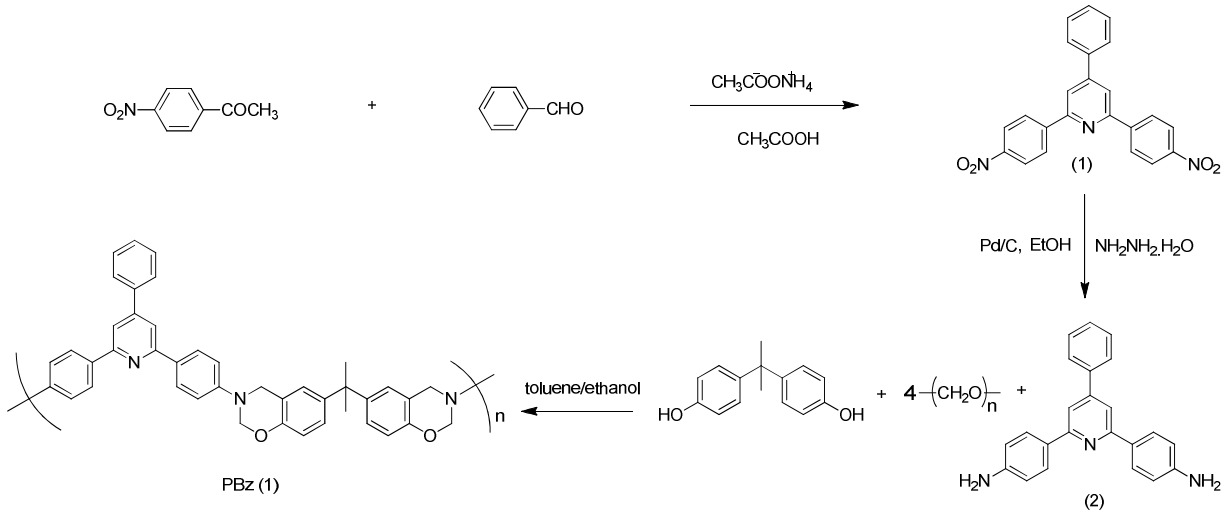

Scheme 1. Synthesis of PBz **(1)**

Table S1 lists the solvent effect on the synthesis of PBz **(1)**. Using homo-solvent, such as 1,4-dioxane (Run 1), chloroform (Run 2), xylene (Run 3), and toluene (Run 4) led to insoluble gelation. Although gelation occurs for PBz **(1)** synthesis in homo-solvent (Run 1-4), the gelation phenomenon was significant improved using toluene/ethanol as reaction solvent (Runs 5-7). A slurry form was obtained for toluene/ethanol (2/1, Run 5). Increasing the ratio of ethanol led to a homogeneous solution (Runs 6-7). Figure S2 shows the NMR trace for PBz **(1)** synthesized in Run 5. A triazine signal at 4.88 ppm was observed after 2 h, and reached a maximum after 4 h. After that, the signal decreased gradually with reaction time. However, residual phenol and triazine signals suggest the reaction was not complete. Figure S3 shows the NMR trace for PBz **(1)** synthesized Run 6. Unlike those shown in Figure S2, no triazine signal was observed. According to literature, preparation of main-chain type polybenzoxazine is proceeded by two steps: the formation of triazine

network (R_1) and the dissociation of the resulting triazine network (R_2).[26] The competition between R_1 and R_2 plays a key role for the preparation. Gelation can occur if reaction rate of R_1 is much faster than that of R_2. In preparing bisphenol/monoamine-based benzoxazine, the gel will react with bisphenol, giving the desired product. However, in preparing diamine/monophenol-based benzoxazine, we found that the decomposition of gel is not as easy as that in preparing bisphenol/monoamine-based benzoxazine. Therefore, reducing R1 is a strategy to prepare diamine/monophenol-based benzoxazine with high yield and purity. The fact that no triazine signal was observed in Figure S3 suggests that reaction rate of R_1 was reduced at a higher ethanol concentration. This result is consistent with our proposal in a previous work that ethanol, which is structurally similar to methylol (-NCH_2OH), solvates the methylol.[24] The solvation hindered the condensation of methylol and hydrogen, and thus reduced the reaction rate of R1. The characteristic oxazine peaks at 5.3 ppm and 4.6 ppm confirm the structure of benzoxazines. No signal was observed corresponding to N-C**H$_2$**-ph at around 4.1 ppm, which resulted from the ring opening of benzoxazine. A further increase in the ethanol ratio led (67%) to a low yield (Run 7). This might be due to the product being somewhat soluble in the precipitation process. Figure S4 shows the ^{1}H-NMR spectrum of PBz **(1)** prepared by Run 6, Table S1. The characteristic oxazine peaks at 4.6 and 5.4 ppm support the structure of PBz **(1)**. In the IR spectrum (not shown), absorptions at 945 cm^{-1} for oxazine, and absorptions at 1032 cm^{-1} (symmetric stretch) and 1232 cm^{-1} (asymmetric stretch) for Ar-O-C were osbserved, supporting the structure of PBz **(1)**. The integral area of methylene in N-C**H$_2$**-ph/methyl in isopropylidiene is 0.48, which is lower than the theoretical value of 0.67. The lower ratio can be explain by the existence some ring-opened structure in the PBz **(1)**. The other possible reason is that PBz **(1)** is phenol-terminated telechelic oligomer with number average moleuclar weight 3500 g/mol (Table 1), and the phenol-terminated structure leads to higher interal area of isopropylidene signals.

Synthesis of PBz (2). Diamine **(5)**, a precursor for PBz **(2)**, was prepared by a three step procedure according to Scheme S1.[25] Figure S5 shows the ^{1}H-NMR spectrum of **(5)**. The assignment is consistent with the structure. PBz **(2)** was prepared from the Mannich condensation of **(5)**, paraformaldehyde, and bisphenol A (Scheme S1 and Runs 8-10 of Table S1). Figure S6 shows the ^{1}H-NMR spectrum of PBz **(2)**. The characteristic oxazine peaks at 4.6 and 5.4 ppm support the structure of PBz **(2)**. While PBz **(1)** shows good solubility during preparation, there was powder precipitation (not gelation) after reacting for 1 h due to the poor solubility of PBz **(2)**. Therefore, the early precipitation lowers the purity of PBz **(2)**, as shown by the residual phenolic OH in Figure S6. Table S2 lists the solubility data of PBz **(1)** and PBz **(2)**. PBz **(1)** was soluble in most organic solvents. In contrast, PBz **(2)** was insoluble in most organic solvents. It was only soluble in NMP at high temperature, but precipitation occurred after cooling. PBz **(2)** is structurally similar to PBz **(1)** except for the pyridinyl group, so the result demonstrates the advantage of pyridinyl group in solubility. The poor solubility of PBz **(2)** makes it difficult to process for property comparison between the thermosets of PBz **(1)** and PBz **(2)**.

Molecular weight of PBz (1). Table 1 lists the GPC and viscosity data of the PBz **(1)**. The number-average molecular weight (M_n) ranges from 2.4×10^3 to 3.5×10^3 g/mol, and the weight-average molecular weight (M_w) ranges from 9.2×10^3 to 1.4×10^4 g/mol for PBz **(1)** prepared in toluene/ethanol. In contrast, M_n ranges from 1.2×10^3 to 1.7×10^3 g/mol, and M_w ranges from 3.5×10^3 to 4.3×10^3 g/mol for PBz **(1)** prepared in xylene and toluene. The inherent viscosities of PBz **(1)** prepared in toluene/ethanol were in the range of 0.14-0.17 dL/g, which are higher than those (0.10-0.12 dL/g,) prepared in xylene and toluene. The GPC and viscosity data demonstrate the advantage of toluene/ethanol in preparing PBz **(1)** with higher molecular weight.

Table 1. Molecular weight and viscosity of PBz **(1)**

Sample ID	Preparation solvent	Yield (%)	Inherent viscosity (dL g^{-1}) [a]	M_w	M_n	PDI
PBz (**1**)	xylene[b]	30	0.10	3.5×10^3	1.2×10^3	3.01
PBz (**1**)	Toluene[c]	35	0.12	4.3×10^3	1.7×10^3	2.51
PBz (**1**)	toluene/ethanol (2/1)[d]	70	0.14	9.2×10^3	2.4×10^3	3.75
PBz (**1**)	toluene/ethanol (1/1)[e]	80	0.17	1.4×10^4	3.5×10^3	3.93

[a] 0.5 gdL^{-1} in NMP at 30 °C.

[b] Prepared by Run 3, Table S1. Note that PBz **(1)** was obtained from the precipitation of its xylene solution into n-hexane. The gelation part was not included in the precipitation.

[c] Prepared by Run 4, Table S1. Note that PBz **(1)** was obtained from the precipitation of its toluene solution into n-hexane. The gelation part was not included in the precipitation.

[b] Prepared by Run 5, Table S1.

[b] Prepared by Run 6, Table S1.

UV-Vis characteristic of PBz (1). Figure 1 shows the UV–vis spectra of PBz **(1)** and protonated PBz **(1)** in a THF dilute solution (10^{-2} M). PBz **(1)** displays an absorption at 338 due to the π-π* transition of unpaired electrons of the pyridinyl group. When the THF dilute solution of PBz **(1)** was protonated with HCl, the intensity at 338 nm decreased due to the lone pair of electrons of the pyridinyl group was quaternized by HCl. A new absorption at 458 nm for a lower π-π* transition of the quaternated PBz **(1)** appeared when the concentration of HCl was higher than 0.1 M. Figure 2 shows the photos of PBz **(1)** and protonated PBz **(1)** in a THF dilute solution. The THF solution of protonated PBz **(1)** shows yellow color, complementary colors of the absorption at 458 nm. The spectroscopic data suggests PBz **(1)** can be used as a proton sensor via a protonation process.

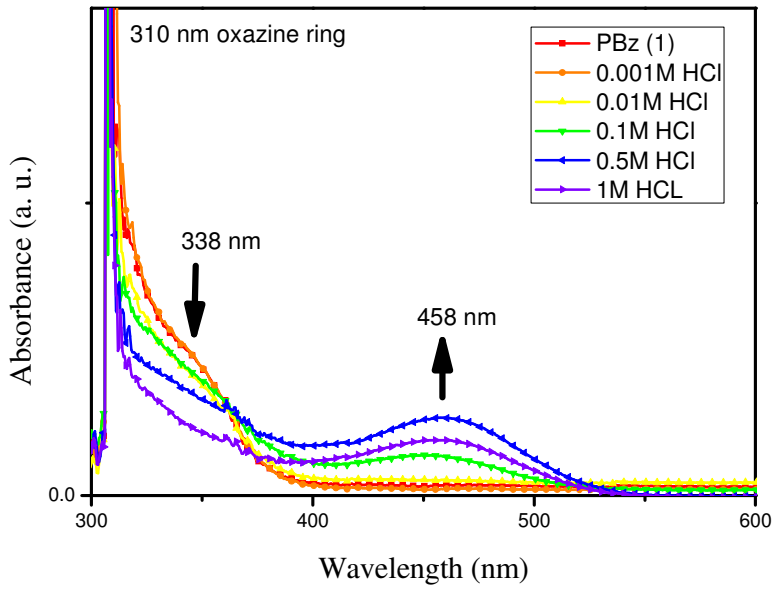

Figure 1. UV-vis Absorption spectra of PBz **(1)** and protonated PBz **(1)** in a THF dilute solution (10^{-2} M)

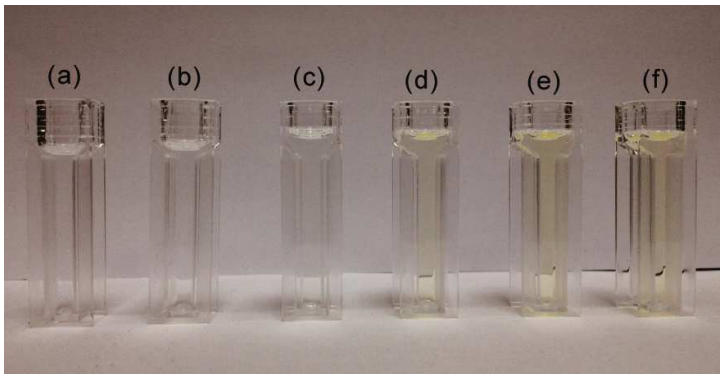

Figure 2. Photos of THF dilute solution of (a) PBz **(1)**, and protonated PBz **(1)** with HCl (b) 0.001M (c) 0.01M (d) 0.1M (e) 0.5M and (f) 1.0 M.

Emission characteristic of PBz (1). Figure 3 shows the emission spectra of PBz **(1)** and protonated PBz **(1)** after being excited at 458 nm. No obvious fluorescence at 500-700 nm was observed in the fluorescence spectrum for PBz **(1)**. However, a new strong fluorescence at 570 nm that increased with the concentration of HCl was observed. The spectroscopic data suggest that the emission is a lower transition related to the protonated pyridinyl group. Interestingly, the emission intensity

increased with the concentration of HCl when the concentration was below 0.5 M, and decreased when the concentration reached 1.0 M. Before protonation, both pyridinyl and benzoxazine groups were donors, so no emission occurred after excitation. The speculation for the phenomenon was proposed as following. On protonation at low HCl concentration, the protonation occurred at the pyridinyl, as shown by PBz **(1)**-H in Scheme 3, since the nitrogen of the pyridinyl group is more basic than that of benzoxazine. The protonated pyridinyl became a stronger acceptor, and then an emission at 570 nm occurred between the nitrogen of benzoxazine (donor) and the protonated pyridinyl groups (acceptor). On protonation at higher HCl concentration, the nitrogen of benzoxazine was protonated, as shown by PBz **(1)**-2H in Scheme 3, changing the benzoxazine from a donor to a weak acceptor. In this case, both the protonated pyridinyl and protonated benzoxazine groups were donors, so no emission occurred after excitation. This explains the decreased emission of protonated PBZ **(1)** at HCl concentration higher than 0.5 M.

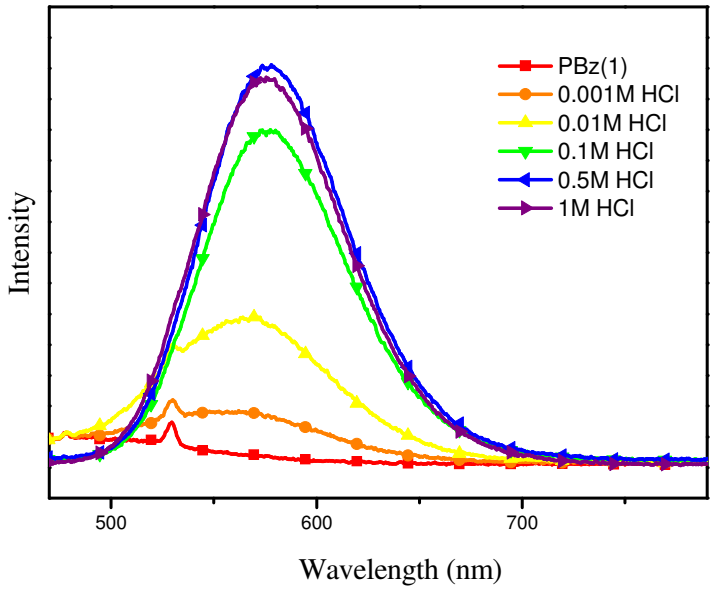

Figure 3. Emission spectra of THF dilute solution of PBz **(1)** and protonated PBz **(1)** after being excited at 458 nm

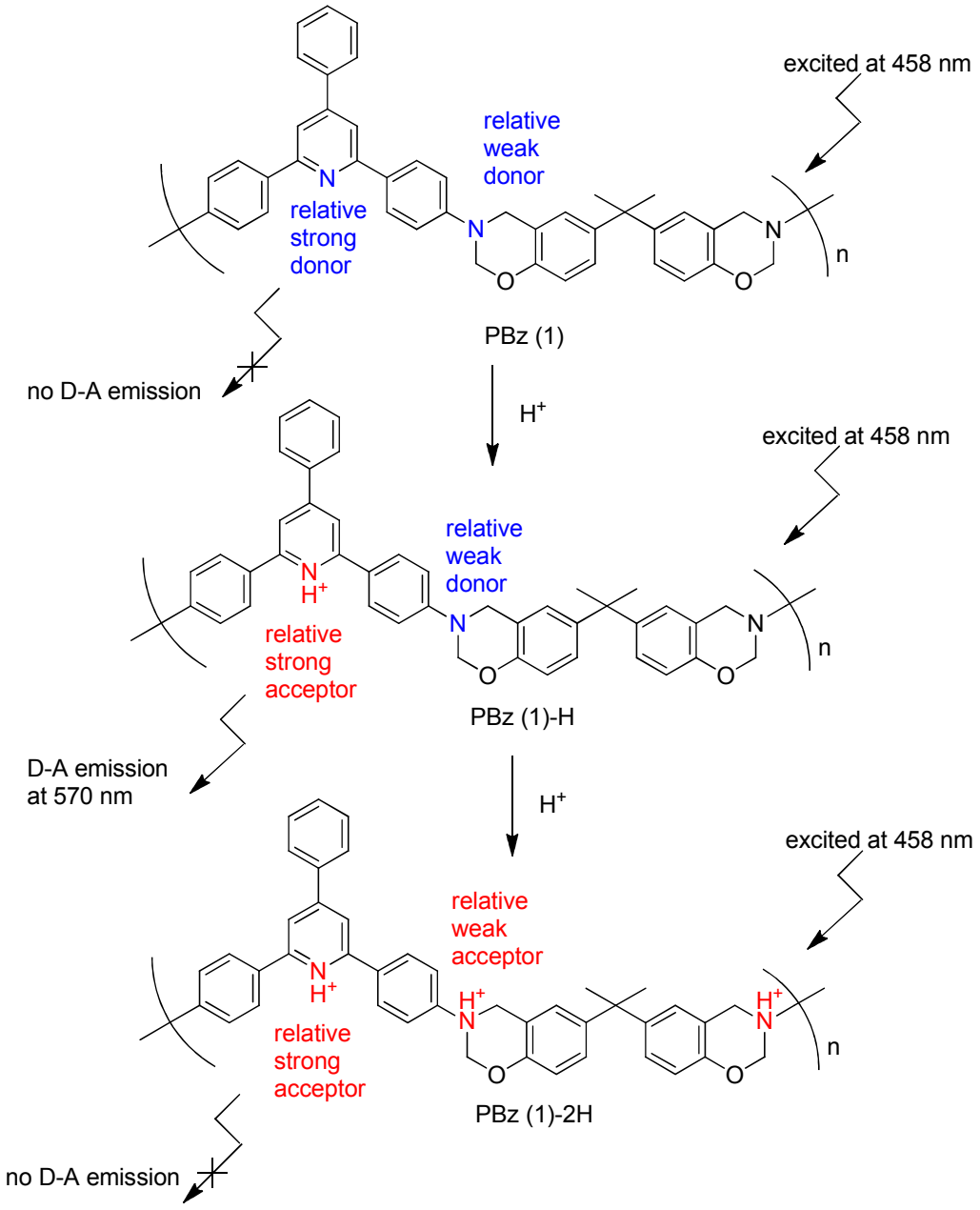

Scheme 3. The proposed structure for the protonated PBz (**1**).

Figure S7 shows the emission spectra of P(B-oda) and protonated P(B-oda) in THF dilute solution. Note that P(B-oda) is a main-chain type polybenzoxazine prepared from 4,4'-diamino diphenyl methane/phenol/paraformaldehyde. No obvious emission was observed (the longitudinal scale is the same as that in Figure 3) for either P(B-oda) or protonated P(B-oda), in which no pyridinyl group was present. The spectroscopic data further supports that the emission in Figure 3 is relative to the

protonated pyridinyl group. The result further suggests that the pyridinyl-containing PBz **(1)** can be used as a proton sensor via a protonation process.

Thermal properties of PBz (1) thermoset. PBz **(1)** was thermally cured to PBz **(1)** thermoset, the PBz **(1)**-T. Figure S8 shows a photo of PBz **(1)**-T at a thickness of 60 um and 550 um. The film of PBz **(1)**-T can be bent even with dimensions as small as 60 μm× 2.5 cm× 0.8 cm. The thermal properties of PBz **(1)**-T were evaluated by DMA and TMA. Figure S9 shows the DMA thermograms of the PBz **(1)**-T. The T_g obtained from the peak temperature of tan δ was 261 ^oC. Takeichi et al. reported that the T_g of pyridinyl-containing benzoxaine thermoset is 40 ^oC higher than bisphenol A/formaldehyde/aniline-based benzoxazine thermoset due to the strong hydrogen bonding between the pyridinyl moiety and phenolic group.[27] However, no PBz **(2)**-T data are available for property comparison because of the poor solubility of PBz **(2)** in organic solvents. The TMA measurement (Figure S10) shows that the T_g value of PBz **(1)**-T is 246 ^oC, and the coefficient of thermal expansions (CTE) is 38 ppm/^oC, which is a relative lower one compared with other benzoxazine thermosets. Figure S11 shows the TGA thermograms of the PBz **(1)**-T. The 5% degradation temperature is 414 ^oC in nitrogen, and 418 ^oC in air. The char yield at 800 ^oC is 56 in nitrogen, and 47 in air. These values are relatively high when compared with other benzoxazine thermosets. Unfortunately, PBz **(2)**, which is structurally similar to PBz **(1)** except for the pyridinyl, was insoluble in solvent for film formation. Therefore, the effect of pyridinyl on thermal properties was not available.

Dielectric properties of PBz (1)-T. The dielectric constant of the PBz **(1)**-T was measured by an Agilent E4991A RF Impedance Material Analyzer. The dielectric constant at 1 GHz and 100 MHz was 3.77 and 3.91, respectively. The value is much higher than fluorinated polybenzoxazines, and is relatively higher than that of P-oda, and F-a thermosets.[28] Note that P-oda is a benzoxazine based on 4,4'-diamino diphenyl methane/phenol/paraformaldehyde, and F-a is a benozoxazine based on

bisphenol F/aniline/paraformaldehyde. Liaw *et al.* reported the dielectric constant of poly(pyridine imide) at 1 kHz (4.20) was higher than that of the commercially available polyimide film Kapton HN (3.50 at 1 kHz).[4, 6] Hougham *et al.* reported that the dielectric constant is affected by a molecule's hydrophobicity and free volume, and polarizability.[29] The pyridinyl group that increases the polarizability of a polymer under an electrical field is thought to be responsible for the increased dielectric constant.

Contact angle and surface free energy of PBZ (1)-T. Figure 4 shows the contact angle of water for PBz **(1)** after curing at 240 ^{o}C for (a) 0, (b) 1, (c) 4, and (d) 8 h. Table 2 lists the data of contact angles and the surface free energies of all tested specimens after various curing times at 240 °C. Although the surface free energy of a solid can be used as a guide or indicator of its relative adhesive properties, it is difficult to measure the surface free energy of a solid directly. For practical reasons, procedures based on contact angle measurements are commonly employed.[30, 31] We evaluated the surface free energies using van Oss and Good's three-liquid method.[32] Table 2 lists the relationship between the surface free energy and the curing time. The surface free energy initially decreased and then increased steadily with the increase in curing time. The lowest value of surface free energies of PBz **(1)**-T was 19.6 mJ/m^2, which is less than that of pure Teflon (21.0 mJ/m^2) when using the same testing liquids and calculation method.[33]

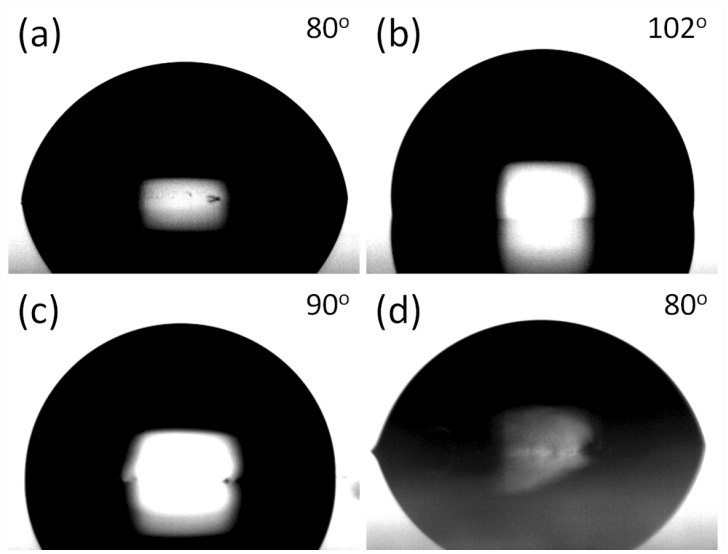

Figure 4. The contact angle of water for PBz **(1)** after curing at 240 °C for (a) 0, (b) 1, (c) 4, and (d) 8 h.

Table 2. The contact angles for water, ethylene glycol (EG) and diiodomethane (DIM) on PBz **(1)** film (standard deviations in the range 0.3－2.0). The corresponding surface free energies and fraction of intermolecular hydrogen bonding are also given.

Temp.	Time	Contact angle (°)			Surface free energy	Fraction of intermolecular
(°C)	(h)	H_2O	EG	DIM	(mJ/m^2)	hydrogen bonding (%)
60	1	80.1	60.0	30.3	44.2	--
	1	102.2	83.4	77.0	19.6	34.7
240	4	91.5	76.2	75.6	21.7	41.3
	8	80.3	65.2	72.5	26.0	47.9

Previous studies[18, 34-36] have suggested that an increase in the degree of intramolecular hydrogen bonding will decrease the surface energy of a polymeric material. To determine the degrees of hydrogen bonding with these polybenzoxazines, we performed curve-resolving of their FTIR spectra with respect to the corresponding frequencies of each hydrogen bonding species. Figure 5 displays expand FTIR spectra (4000－2000 cm^{-1}) for the PBz **(1)** curing at 240 °C for (a) 1 h, (b) 4 h, and (c) 8 h. Four different kinds of hydrogen bonds were evident: $—O^{-}\cdots H^{+}N$ intramolecular hydrogen

bonds (2830 cm^{-1}), −OH···N (from Mannich bridge) intramolecular hydrogen bonds (3171 cm^{-1}), −OH···O and −OH···N (from pyridinyl) intermolecular hydrogen bonds (3400−3370 cm^{-1}), and −OH···π intramolecular hydrogen bonds (3550 cm^{-1}), which have been discussed in previous reports.[27, 37] The peak at 3380 cm^{-1} corresponds to the intermolecular hydrogen bonding of the polybenzoxazine, and it is clear that the fraction of these intermolecular hydrogen bonds increased upon increasing the curing time (Table 2). Wang and Chang et al. reported that the curing time influences the surface free energy of polybenzoxazines; they found that the lowest surface free energy occurred when the system possesses the minimal extent of −OH···O intermolecular hydrogen bonding.[18] The area fraction of these hydrogen bonds increased upon increasing the curing time. It is clear that increasing the degree of intramolecular hydrogen bonding will lead to a decrease in the surface free energy, whereas increasing the fraction of intermolecular hydrogen bonding has the opposite effect. Our observations are in a good agreement with the results of previous studies on surface free energy effects[18, 24, 34-36] As shown in Table 2, the fraction of intermolecular hydrogen bonding is 34-48%, which is much higher than that in our previous work.[16, 19, 27-29] The hydrogen bonding between the phenolic OH and pyridinyl moiety is responsible for the increased fraction. However, high contact angle (102^{o}) and low surface energy (19.6 mJ/m^2) can still be obtained even with the high Fraction of intermolecular hydrogen bonding. This phenomenon has never been reported.

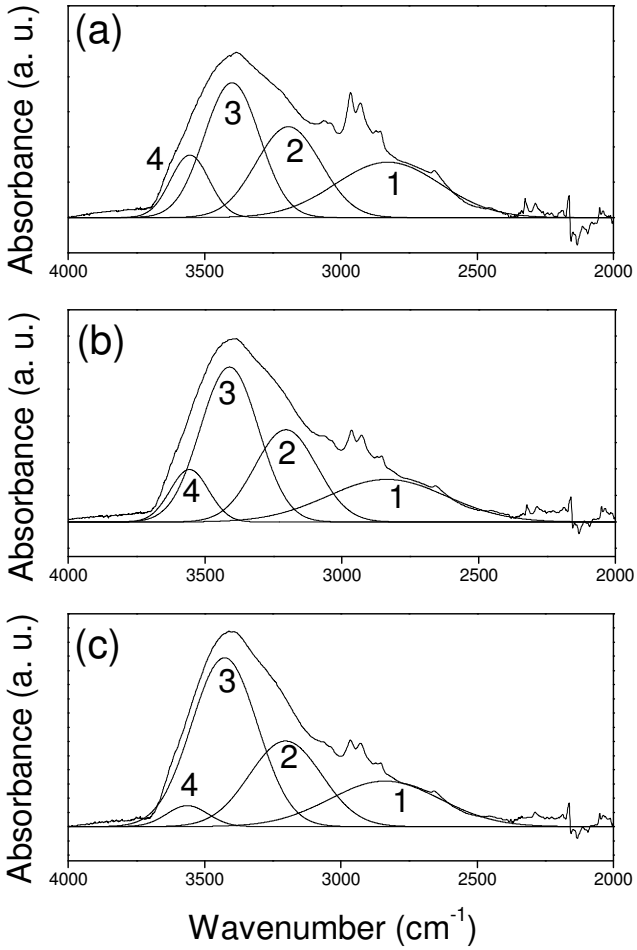

Figure 5. Curve fitting of the FTIR spectra of PBz **(1)** curing at 240 °C for (a) 1 h, (b) 4 h and (c) 8 h. 1: —$O^{-}\cdots H^{+}N$ intramolecular hydrogen bonding. 2: — OH···N (from Mannich bridge) intramolecular hydrogen bonding. 3: —OH···O and —OH···N(from pyridinyl) intermolecular hydrogen bonding. 4: —OH···π intramolecular hydrogen bonding.

Conclusions

We have successfully prepared a pyridinyl-containing polybenzoxazines, PBz **(1)**, from the Mannich condensation of **(2)**, phenol, and paraformaldehyde using toluene/ethanol (1/1) as the reaction solvent. When the THF dilute solution of PBz **(1)** was protonated with HCl, the intensity at 338 nm decreased, and a new absorption at 458 nm appeared in the UV-vis spectra. No obvious fluorescence at 500-700 nm was observed in the emission spectrum for PBz **(1)**. However, a new strong fluorescence at 570 nm was observed in the emission spectrum for protonated PBz **(1)**. In contrast, no obvious emission was observed for either P(B-oda) or protonated P(B-oda), in which no pyridinyl group was present. These results suggest that the pyridinyl-containing PBz **(1)** can be used as a proton sensor via a protonation process. To the best of our knowledge, the absorption and emission of protonated polybenzoxazines has not been reported. After curing, the thermoset of PBz **(1)**, PBz **(1)**-T, shows a T_g value at 261 ^oC, and a CTE at 38 ppm/^oC, and 5% decomposition temperature at 414 (N_2) and 419 ^oC (air), demonstrating moderate-to-high thermal stability. FTIR spectra show that the surface free energy is strongly related with the fraction of intermolecular hydrogen bonding. In addition, the fraction of intermolecular hydrogen bonding in this work is much higher than that in our previous work due to the hydrogen bonding between the phenolic OH and pyridinyl moiety. However, high contact angle (102^o) and low surface energy (19.6 mJ/m^2) can still be obtained even with the high Fraction of intermolecular hydrogen bonding.

Acknowledgment. The authors thank the National Science Council of the Republic of China for financial support.

Notes and references

1. B. Tamami and H. Yeganeh, *Polymer*, 2001, **42**, 415-420.
2. K.-L. Wang, W.-T. Liou, D.-J. Liaw and S.-T. Huang, *Polymer*, 2008, **49**, 1538-1546.
3. B. Tamami and H. Yeganeh, *Journal of Polymer Science Part A: Polymer Chemistry*, 2001, **39**, 3826-3831.
4. D.-J. Liaw, K.-L. Wang, F.-C. Chang, K.-R. Lee and J.-Y. Lai, *Journal of Polymer Science Part A: Polymer Chemistry*, 2007, **45**, 2367-2374.
5. X. Wang, Y. Li, C. Gong, S. Zhang and T. Ma, *Journal of Applied Polymer Science*, 2007, **104**, 212-219.
6. D.-J. Liaw, K.-L. Wang and F.-C. Chang, *Macromolecules*, 2007, **40**, 3568-3574.
7. A. Chichibabin and O. Zeide, *Zhur. Russ. Fiz. Khim. Obshch (J. Russ. Phys. Chem. Soc.)*, 1914, **46**, 1212.
8. R. L. Frank and R. P. Seven, *Journal of the American Chemical Society*, 1949, **71**, 2629-2635.
9. J. J. Li, in *Name Reactions*, Springer, 2009, pp. 107-109.
10. A. Katritzky and C. Rees, *Comprehensive Heterocyclic Chemistry, Vol. 2, p395*, Pergamon, Oxford, 1984.
11. M. Weiss, *Journal of the American Chemical Society*, 1952, **74**, 200-202.
12. Y.-C. Huang, K.-L. Wang, C.-H. Chang, Y.-A. Liao, D.-J. Liaw, K.-R. Lee and J.-Y. Lai, *Macromolecules*, 2013, **10.1021/ma4013972**.
13. D.-J. Liaw, K.-L. Wang, E.-T. Kang, S. P. Pujari, M.-H. Chen, Y.-C. Huang, B.-C. Tao, K.-R. Lee and J.-Y. Lai, *Journal of Polymer Science Part A: Polymer Chemistry*, 2009, **47**, 991-1002.
14. N. N. Ghosh, B. Kiskan and Y. Yagci, *Progress in Polymer Science*, 2007, **32**, 1344-1391.
15. K. Zhang, Q. Zhuang, X. Liu, R. Cai, G. Yang and Z. Han, *RSC Advances*, 2013, **3**, 5261-5270.
16. P. Zhao, Q. Zhou, Y. Deng, R. Zhu and Y. Gu, *RSC Advances*, 2013, **10.1039/C3RA44738C**.
17. X. Ning and H. Ishida, *Journal of Polymer Science Part A: Polymer Chemistry*, 1994, **32**, 1121-1129.
18. C.-F. Wang, Y.-C. Su, S.-W. Kuo, C.-F. Huang, Y.-C. Sheen and F.-C. Chang, *Angewandte Chemie International Edition*, 2006, **45**, 2248-2251.
19. T. Takeichi, T. Kano and T. Agag, *Polymer*, 2005, **46**, 12172-12180.
20. T. Agag and T. Takeichi, *Journal of Polymer Science Part A: Polymer Chemistry*, 2007, **45**, 1878-1888.
21. J. Liu, T. Agag and H. Ishida, *Polymer*, 2010, **51**, 5688-5694.
22. T. Agag, S. Geiger, S. M. Alhassan, S. Qutubuddin and H. Ishida, *Macromolecules*, 2010, **43**, 7122-7127.
23. C. Altinkok, B. Kiskan and Y. Yagci, *Journal of Polymer Science Part A: Polymer Chemistry*, 2011, **49**, 2445-2450.
24. C. H. Lin, S. L. Chang, T. Y. Shen, Y. S. Shih, H. T. Lin and C. F. Wang, *Polymer Chemistry*, 2012, **3**, 935-945.
25. I. K. Spiliopoulos and J. A. Mikroyannidis, *Macromolecules*, 1998, **31**, 1236-1245.
26. Z. Brunovska, J. P. Liu and H. Ishida, *Macromolecular Chemistry and Physics*, 1999, **200**, 1745-1752.
27. Y. Shibayama, T. Kawauchi and T. Takeichi, *High Performance Polymers*, 2013, **10.1177/0954008313495245**.
28. C. H. Lin, S. L. Chang, H. H. Lee, H. C. Chang, K. Y. Hwang, A. P. Tu and W. C. Su, *Journal of Polymer Science Part A: Polymer Chemistry*, 2008, **46**, 4970-4983.
29. G. Hougham, G. Tesoro and J. Shaw, *Macromolecules*, 1994, **27**, 3642-3649.

30. F. M. Fowkes, *The Journal of Physical Chemistry*, 1962, **66**, 382-382.
31. W. A. Zisman, *Industrial & Engineering Chemistry*, 1963, **55**, 18-38.
32. C. J. Van Oss, M. K. Chaudhury and R. J. Good, *Chemical Reviews*, 1988, **88**, 927-941.
33. J. Tsibouklis, M. Stone, A. A. Thorpe, P. Graham, T. G. Nevell and R. J. Ewen, *Langmuir*, 1999, **15**, 7076-7079.
34. S.-W. Kuo, Y.-C. Wu, C.-F. Wang and K.-U. Jeong, *The Journal of Physical Chemistry C*, 2009, **113**, 20666-20673.
35. H.-C. Lin, C.-F. Wang, S.-W. Kuo, P.-H. Tung, C.-F. Huang, C.-H. Lin and F.-C. Chang, *The Journal of Physical Chemistry B*, 2007, **111**, 3404-3410.
36. L. Qu and Z. Xin, *Langmuir*, 2011, **27**, 8365-8370.
37. H.-D. Kim and H. Ishida, *The Journal of Physical Chemistry A*, 2001, **106**, 3271-3280.